International Journal for Multidisciplinary Research (IJFMR)
E-ISSN: 2582-2160 ● Website: www.ijfmr.com ● Email: editor@ijfmr.com

Load Frequency Control of RES Interconnected Two area Power Systems Using Fractional Order Controller

Suraj Kumar[1], Sanjeev Kumar Bhagat[2], Pooja Jha[3]

[1]PG Scholar, Electrical Engineering, Sandip University
[2]Assistant Professor, Electrical Engineering, Sandip University
[3]Assistant Professor (H.O.D), Electrical Engineering, Sandip University

Abstract
This study presents a fractional order load frequency control scheme for a renewable energy integrated two-area interconnected power system. The increasing penetration of photovoltaic and wind generation introduces low inertia and uncertainty, which degrade frequency stability under sudden load variations. To address this challenge, a Grasshopper Optimization Algorithm tuned fractional order proportional integral derivative controller is proposed. The dynamic model incorporates virtual inertia support, tie-line power exchange, and realistic governor–turbine dynamics. The performance of the proposed controller is compared with several techniques from the existing literature under different operating scenarios. Simulation results demonstrate significant reduction in frequency deviation, tie-line power oscillations, settling time, and integral squared error, confirming the suitability of the proposed method for reliable frequency regulation in modern renewable dominated grids.

Keywords: Frequency Control, Fractional Order PID, Renewable Energy Integration, Grasshopper Optimization Algorithm, Virtual Inertia, Two-Area Power System.

1. Introduction

Reduced load on the power system during peak hours and cost savings for customers are two of the many major benefits of using renewable energy sources (RES) to encourage clean energy use and minimize greenhouse gas (GHG) emissions. A growing amount of electric energy is coming from renewable sources, such as photovoltaic grids, which are electrically linked with load frequency controls (LFCs) of interconnected parts of power systems to ensure the sustainability and stability of such systems. Existing models of electricity production are made more unpredictable and variable by the addition of PV to the system. Each of the several regions that make up an interconnected power system is responsible for generating enough electricity to satisfy the load demands of its consumers while simultaneously maintaining a certain system frequency and interchanged power setpoint [1]. In order to avoid steady-state errors induced by frequency transients, the LFC for area 1 is designed to compensate for governor droop [2]. In order to minimize errors in steady state, LFC must be operated with a traditional proportional integral derivative (PID) controller. When power systems are linked, LFC studies are a crucial component [3]. By modifying the generator output to meet the demand side, LFC ensures that the system frequency maintains at a nominal value of 50 Hz and links the producing site and

the demand side in real-time, making it an essential function in the power system. In order to maintain the system frequency and the corresponding power angle at pre-set values, the synchronous generators speed up or slowdown in the control zone as described in [4,5] under both static and dynamic situations. Deviation from the nominal frequency set point is fluctuating within a range of plus or minus 0.1 Hz, as stated in [6]. However, due to the fact that they need to adhere to frequency regulations in order to integrate seamlessly with existing power systems, there are always concerns and obstacles with their implementation [7].

When it is not possible to manually operate an interconnected power system (PS), the most significant problem is regulating the frequency and tie-line power [8]. Accurately matching the produced power to the load in a nominal condition is also a difficult challenge to solve [9, 10]. An automated generation control (AGC) system may automatically operate the turbine's valve or gate position to compensate for this imbalance. The turbine's water or steam input must be controlled precisely so it can meet the actual power requirement [11]. An approach to managing power and frequency in relation to one another is provided by prime mover governing systems, which is sometimes abbreviated as AGC or LFC. Separating the whole system into several control zones is a common practice in AGC studies of large, complex, linked PSs. When all of the PS components' generators are in a control area and running at the same frequency, it's called a control area. In a typical steady-state operation, the control area maintains the power requirement of each region and the overall frequency of the system [13].

Each control area maintains its frequency and tie-line power during load perturbations by reducing the area control error (ACE), which is a combination of frequency and tie-line power variations. Recent years have been research on AGC of multi-area systems with an eye toward multi-control regions. Mainly, they want to maintain the set levels of frequency and tie-line power. The LFC loop keeps the frequency, the speed of the governor, and power output constant. The main loop and the secondary loop make up this LFC loop, which operates independently of each other. The main control loop is quicker and reacts to signals of frequency. The secondary loop, in contrast, is a slower loop that handles fine-grained frequency modifications and guarantees correct megawatt exchange among various control regions. This, in contrast to the main loop, is unresponsive to abrupt changes in frequency and tiepower deviations. The secondary loop is initiated after the first loop has finished its duty. Therefore, AGC control loops can only be operated effectively with well-designed controllers. Suppressing the undesired deviations and regulating ACE to zero requires a good secondary controller. As shown in Figure 1 [13], the AGC system is made up of the LFC and the automated voltage regulator loop.

Figure 1: AGC with LFC and AVR loops

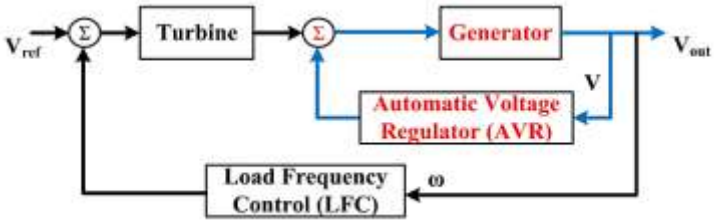

Reactive power compensation and other aspects of PV grid integration have been the subject of many recent studies that aim to increase power system dependability. To regulate PV integration inverters to the grid for performance standards and power quality, writers have been delving deeply into the new

standard grid codes in [14, 15]. In [16], the authors revealed that when paired with the AVR model for a two-area interconnected power system, the suggested LFC technique yields superior dynamic responsiveness. In [17], the authors discuss how to build isolated microgrid frequency controllers that use droop and voltage control to improve the system's stability, resilience to severe disturbances, and frequency responsiveness. They also mention how to use the fuzzy logic controller algorithm (FLC). Parameter variation excitation control, an appropriate power system profile, and a control performance of a load frequency control (LFC) regulation are all covered in [18]. In addition, fractional calculus has found widespread use in control systems, namely in the controller's ability to make use of fractional order differentiation and integration [19]. It applies real, complex, variable, or distributed order operators to standard integer order calculus, making it more general.

Due to its resilience in the face of plant gain changes and uncertainty, fractional controllers have recently become more common. Controls of fractional order (FO) provide for greater leeway in adjusting design criteria like phase margins and gain than controllers of integer order (IO).

More robustness than extremely high-order IO controllers is achieved by the FO controller with fewer tuning knobs [20]. The fractional operators, also known as differintegrals, are able to remember their previous states, which enhances their filtering capabilities. Less control effort is required because to this attribute. Therefore, a FO controller produces a more consistent control signal than an IO controller [21]. With more parameters available with FO controllers compared to IO controllers, more design standards may be fulfilled. Consequently, fractional control allows for the creation of control systems that are more resilient and accurate. Power electrical system control and modeling utilizing fractional calculus has shown tremendous progress in the last decade. Two of the most popular types of controllers utilized in this field are proportional integral (PI) and proportional integral derivative (PID). There has been a lot of recent research on fractional-order PI/PID controllers for electric and hybrid vehicles, microgrids, maximum power point tracking (MPPT) control of photovoltaic panels, electrical drives, grid-connected and/or photovoltaic inverters, and wind energy applications with multi-level converters [22, 23].

Results from simulations and hardware implementations demonstrate that fractional control outperforms conventional controllers when applied to power electronic systems [24]. But the main problem with low-inertia is that high-penetration RESs integrate them, thus current LFC methods may not be enough to deal with it. As a result, this research suggests a GOA-FOPID controller for the LFC of a two-area linked contemporary power system as a solution to this problem.

A. Background

Integrals and derivatives of integer order (d/d^x, $d\ 2/d^{x2}$, etc.) are the focus of traditional calculus. Partiality calculus emerged from a seventeenth-century debate between Leibniz and L'Hopital over the prospect of non-integer order in calculus [25]. A significant number of distinguished mathematicians have since worked to advance fractional calculus [26].

In fractional calculus, the continuous integrodifferential operator cD α t is defined, where α indicates the order of operation, which may be real or complex, c and t denote the limits of the operation, and R(α) represents the real portion of A. Differentiation and integration are both handled by this operator [27].

$$ {}_cD_t^{\alpha} = \begin{cases} \frac{d^{\alpha}}{dt^{\alpha}}; & R(\alpha) > 0 \\ 1; & \alpha = 0 \\ \int_c^t (d\tau)^{-\alpha}; & R(\alpha) < 0 \end{cases} $$

While many have attempted to define fractional calculus, the three most well-known are the ones put out by Grunwald-Letnikov, Riemann-Liouville (RL), and Caputo [25].

Grunwald-Letnikov definition

$$ {}_cD_t^{\alpha}(f(t)) = \lim_{h\to 0} \frac{1}{h^{\alpha}} \sum_{r=0}^{[(\frac{t-c}{h})]} (-1)^r \binom{\alpha}{r} f(t-rh) $$

In this case, the integer component is denoted by [.], and the combination is classified as:

$$ \binom{\alpha}{r} = \frac{\Gamma(\alpha+1)}{\Gamma(r+1)\Gamma(\alpha-r+1)} $$

The Gamma (Γ) function, which is defined as [28], plays a critical role in fractional calculus.

$$ \Gamma(x) = \int_0^{\infty} t^{x-1} e^{-t} dt; R(x) > 0 $$

Riemann-Liouville definition

$$ {}_cD_t^{\alpha}(f(t)) = D^n J^{n-\alpha}(f(t)) $$

$$ {}_cD_t^{\alpha}(f(t)) = \frac{1}{\Gamma(n-\alpha)} \left(\frac{d}{dt}\right)^n \int_c^t \frac{f(\tau)}{(t-\tau)^{\alpha-n+1}} d\tau $$

In this case, "the fractional integral operator J is defined, where n is an integer and α is a real number such that n − 1 < α < n." The operator D −n is often seen being used to the operator J n as well [29].

Caputo's definition

The limits of integration are denoted by {c, t} and α is a fractional order such as 0.5 in both the Riemann-Liouville and Caputo formulations, where n is an integer such that n − 1 < α < n. The Caputo concept employs physically realizable integer-order beginning conditions, making it a more practical and real-world interpretation. According to the Caputo definition, a constant's fractional derivative is zero, but according to the RL definition, it's not [29]. Its definition is

$$ {}_cD_t^{\alpha}(f(t)) = \frac{1}{\Gamma(n-\alpha)} \int_c^t \frac{f^n(\tau)}{(t-\tau)^{\alpha-n+1}} d\tau $$

Because the transfer function contains irrational terms, fractional-order systems have unbounded memory and may be thought of as infinite-dimensional filters. Systems of the integer order, which have limited memory, are a subset of the non-integer order. Therefore, approximations of integer order are necessary for the realistic implementations of fractional order systems. For direct implementation with digital signal processors, digital approximation approaches are favored over analog approximation methods. The Oustaloup CRONE approximation, Carlson's approximation, Charef's approach, Matsuda's method, and many more are examples of famous approximation methods. Both the Grunwald-Letnikoff and the Tustin approximations are used for discrete-time approximations. References [30], [31] provide an overview of approximation methods. The CRONE (CommandeRobusted'Ordre Non Entier) is the approximation that is most often employed. It approximates the fractional operator s α [31] as:

$$ s^{\alpha} \approx C \prod_{i=1}^{N} \frac{1+(s/\omega_{z,i})}{1+(s/\omega_{p,i})} $$

Within the given frequency range {ωl, ωh}, the approximation has N poles and N zeros.

$$ \omega_{z,i} = \omega_l \left(\frac{\omega_h}{\omega_l}\right)^{(2i-1-\alpha)/2N} $$

$$ \omega_{p,i} = \omega_l \left(\frac{\omega_h}{\omega_l}\right)^{(2i-1+\alpha)/2N} $$

At 1 rad/s, the CRONE approach modifies the gain C so that the aforementioned expression's magnitude has a gain of 1 or 0 dB. "In this case, the approximation's order is N, and the optimal sites for the poles and zeros are selected across a certain frequency range [31]. Grunwald-Letnikoff and Tustin approximations are used for discrete-time estimates [32]."

Oldham and Spanier definition

In 1974, a definition for fractional calculus was developed by Oldham and Spanier. Equation following shows this mathematical definition.

$$\frac{d^q(\beta x)}{dx^q} = \beta^q \frac{d^q(\beta x)}{d(\beta x)^q}$$

the following is the definition of the β function:

$$\beta(m,n) = \int_0^1 (1-x)^m x^{n-1} dx \qquad m,n \in \mathbb{R}$$

Check out [33] for several other explanations of fractional-order calculus.

B. Fractional-Order Controller

Recent years have seen advancements in controller technology, both in academic and commercial systems, leading to increasingly sophisticated and intricate designs. There has been a lot of focus on the FOPID controllers in prior years. But FOPID controllers, like the integer PID controllers, nevertheless have basic tuning rules and aren't very successful [34]. Because of its practical simplicity, PID controllers are mostly used in industrial applications. In contrast, PID controllers often have their settings fine-tuned by trial and error, testing, or acquired expertise. Despite its ease of use in academic systems, calculating the controller's gain in an industrial system is no picnic due to "the inherent problems of industrial systems, which include uncertainties, nonlinearities, and structural complexity [35]."

Figure 2: Structure of fractional-order PID controller.

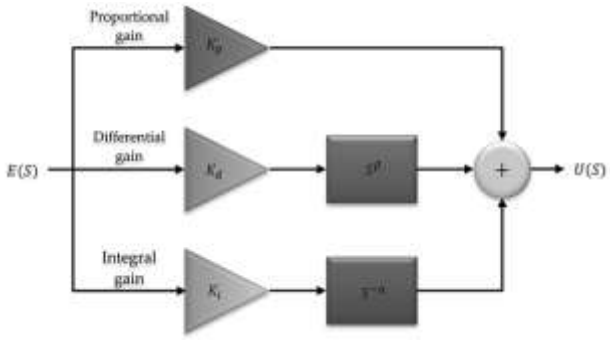

The form of the fractional order that incorporates tilted integral derivative (TID), PID, FOPID, and PD is laid out in detail in [36]. Equation below is used to create the most useful non-entier robust command approximation in this study, which is an alternative to the FOPID controller.

$$S^{\alpha} = C\prod_{i=1}^{n} \frac{1+\left(\frac{s}{\omega_{z,i}}\right)}{1+\left(\frac{s}{\omega_{p,i}}\right)}$$

Even though PID controllers are the most common and useful, FOPID is the domain-of-variations-based alternative. The FOPID controller is more stable than the PID one. When dealing with complicated situations involving several factors, the FO-based controller proves to be the most practical option [37].

Figure 2 shows the schematic of the FO-based PID controller. "The transfer function of fractional-order PID is given in Equation below [37] according to this figure."

$$C(s) = K_p + K_d S^{\beta} + \frac{K_I}{S^{\alpha}}$$

Traditional controllers may be reached by certain values of β and β. "You may change the settings on the proportional controller if β=0 and β=0. The PD controller is activated when β=0 and β=1, even if these parameters have the values β=1 and β=0 in the PI controller. The FOPID controller may be accessed with a flexible character [38] if and only if $\beta \in \mathbb{R}$." Consequently, the FOPID controller is more versatile. Moreover, by intercepting fuzzy logic and adjusting controller settings, the integral of time error is minimized. By merging the genetic algorithm (GA) with the artificial bee colony (ABC) algorithm, a new fractional-order controller with two free degree orders is presented in [39]. The proportional section of PID is substituted with $1/Sn$ to produce the tilted integral derivative. TID is sufficiently strong to mitigate or eliminate disturbance and noise [40].

2. Related Works

In their analysis of the effects of EV integration into two-area thermal systems, Das and Panda (2021) [41] also included the effects of other renewable energy sources. In the absence of integrated vehicle (EV), "the proportional-order proportional integral-fractional-order proportional derivative (FOPI-FOPD) controller, proportional plus integral (PI), proportional plus integral plus derivative (PID), and proportional plus integral-proportional derivative (PI-PD) controller were tested." During the analysis, FOPI-FOPD's superiority over others became very clear. The system with inclusion EVs is thereafter analyzed using the improved FOPI-FOPD controller. To back up the claim that EVs are competent when combined with other renewables, comprehensive simulations and comparisons were presented. A 5% step load perturbation in area1 was considered in the system analysis, and the Sine Cosine Algorithm was used to optimize the controller settings.

In their 2019 publication, Gheisarnejad and Khooban [42] introduced a new controller for the power system called "the fuzzy PIλDF controller, which combines filtered derivative action with a fractional order integrator." This controller is designed "to address the issue of automated generation control (AGC)." The cuckoo optimization algorithm (COA) successfully optimized the parameters of the suggested controller structure. Four commonly used linked test systems were examined in order to evaluate the practicality and utility of the proposed COA optimized fuzzy PIΛDF controller. "These systems include two-area non-reheat thermal, two-area multi-source, three-area thermal, and three-area hydro-thermal power plants." In the model of the three-area power systems, several nonlinearities were included as physical constraints, such as generation rate constraint (GRC) and governor dead band (GDB). This allowed us to test how well the suggested approach handled real-world problems. In order to assess the aforementioned test systems, the uniqueness and acceptability of the COA-based fuzzy PIśDF controller were compared with other previously published methods.

For the purpose of validating their model on both single-area and multi-area power systems, Dey et al. (2021) [43] presented "an equation-based LFC that took into account crucial elements such stator currents, field voltages, damper winding voltages, and network equations, among others." The idea of area interchange control (AIC) was considered while introducing LFC to multi-area linked power system networks. The frequency oscillations and tie-line power variation across various locations were reduced with the use of integral (I), integral derivative (ID), and proportional integral derivative (PID)

controllers. We tuned the controller settings using three distinct meta-heuristic algorithms and compared their results: “Salp swarm algorithms (SSA), Grasshopper optimization algorithm (GOA), and Collective decision optimization algorithm (CDO).” Various load perturbations, including light, medium, and heavy, were also taken into account to ensure that the study was applicable to real-world systems. The results showed that the suggested method was effective, with SSA providing the most optimally adjusted settings for the controllers under consideration.

For the purpose of frequency management in three-area multi-source linked microgrids, Moschos et al. (2023) [44] used a “FOPDF-(1+FOPI) controller that is filtered fractional-order PDF coupled with a one plus fractional-order PI controller.” Using the coot optimization technique, the suggested controller was fine-tuned. Sustainable units, renewable power sources, and hybrid energy storage systems are all part of the planned microgrids. The microgrids, which might be farms or small settlements, relied only on renewable and sustainable energy sources and aimed to show potential configurations for such systems. “The PIDF, integer-order PDF-(1+PI), and FOTDF-(1+TI) controllers were pitted against the suggested controller in a number of situations.” The suggested controller outperformed the second-best option by 29.5% in the first scenario, which comprised testing it in a standalone microgrid. It obtained the highest ITAE rating. Interconnected microgrids across three areas without the use of renewable energy sources were the focus of the second scenario. “If we compare the PIDF and FOTDF-(1+TI) controllers to the FOPDF-(1+FOPI) controller, we find that it cuts the settling time in area one by 79.13% and 52.26%, respectively.”

In their study, Almasoudi et al. (2023) [45] suggested a viable method for effective load frequency control (LFC) that utilizes a fractional-order proportional-integral-derivative-accelerator (FOPIDA-LPF) controller, also known as the PI\DND2N2 controller. The proposed settings for the PIśDND2N2 controller were fine-tuned using a reliable metaheuristic optimization tool called the gray wolf optimizer (GWO). Additionally, a self-contained hybrid maritime microgrid system (HMμGS) with renewable energy sources (RESs), non-sensitive loads, a marine biodiesel generator, and solid oxide fuel cell energy units was constructed to use the proposed PIśDND2N2 controller for its load frequency control (LFC).

In order to improve the frequency stability of contemporary linked power systems, Falehi (2025) [46] set out to build a new “Fractional-Order Interval Type-II Fuzzy Controller (FOIT2FC).” The primary goal of the FOIT2FC design is to reduce frequency and tie-line power variations; however, optimizing its parameters with several objectives may help achieve this goal at the same time. In order to fine-tune the control parameters in the face of step load perturbation and uncertainties related to wind turbines and photovoltaics, “the Multi Objective Path Finder Optimization Algorithm (MOPFOA) was suggested.” Simulated performance of the MOPFOA-based FOIT2FC to reduce frequency and tie-line power variations concurrently has been finally confirmed by the findings.

“The unique LFC approach put out by Sekyere et al. (2024) [47] makes use of a derivative filter (FOPI-FOPIDN) in conjunction with a cascaded fractional-order proportional integral-fractional-order proportional integral derivative.” The FOPI-FOPIDN's parameters were fine-tuned using ADIWACO, a variation of particle swarm optimization (PSO) seen in published works. Performance comparisons with previous LFC control schemes in the literature and thorough simulations on two- and three-area test systems proved the efficacy and scalability of the proposed approach. The ITAE values, power flow variations in the tie-lines, and control area frequency deviations with power systems exposed to various

load and RES generating disturbances in various experimental situations are the performance metrics utilized for assessment.

3. Present Work and Methods

An electricity transmission cable known as the tie-line has linked the two regions. Thermal power plants, loads, and VICs based on ESS are present in every region. Also included in regions 1 and 2, respectively, are photovoltaic (PV) solar farms and wind farms. A wind farm of 6 MW is located in the second region, while an 8 MW solar farm is located in the first. Frequency and tie-line power are handled by the system controller for the two regions. After that, it creates the signals that regulate each section. When trying to simulate the system under investigation, it's possible that the low-order models of the individual generating units are enough for managing the linked power grid. As illustrated in Figure 3, the two-area linked power system that was evaluated makes use of VIC technology. On top of that, Figure 4 displays the model parameters.

Figure 3: Proposed two-area interconnected power system.

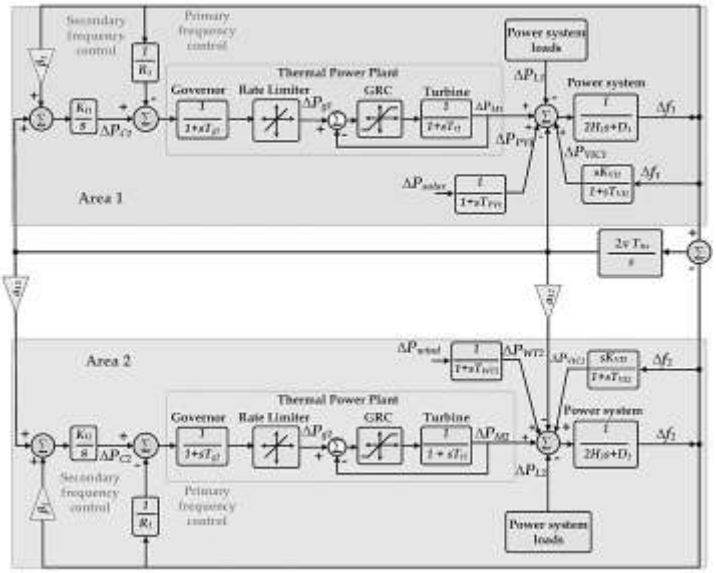

Figure 4: Model's Technical Parameters

Technical Parameter	Area1	Area2
System damping coefficient, D (pu)	0.015	0.016
System inertia, H (pu)	0.083	0.101
The time constant of the governor, T_g (s)	0.080	0.060
The time constant of the turbine, T_t (s)	0.400	0.440
Droop constant, R (pu)	3.000	2.730
Integral control variable gain, K_I	0.300	0.200
Frequency bias factor, β (pu MW/Hz)	0.3483	0.3827
The time constant of the PV system, T_{PV} (s)	1.300	–
The time constant of the WT system, T_{WT} (s)	–	1.500
Virtual inertia control gain, K_{VI} (s)	1.540	1.750
Virtual inertia time constant, T_{VI} (s)	10.000	10.000
Nominal system frequency, f (Hz)	50.000	50.000
Synchronizing coefficient between two areas, T_{tie}	0.080	0.080
The capacity ratio between two areas, α_{12}	−0.600	−0.600

Figure 4 presents the technical parameters adopted for modelling the two-area interconnected power system used in this study. The values of system damping coefficient, inertia constant, governor and turbine time constants define the dynamic behaviour of both areas and directly influence frequency

stability after load disturbances. The inclusion of photovoltaic and wind system time constants represents the impact of renewable energy penetration on area dynamics. Virtual inertia control gain and time constant indicate the support provided by energy storage to emulate conventional generator response. Synchronizing coefficient and capacity ratio describe the strength of tie-line coupling between areas and determine power exchange capability during transient conditions.

Figure 5: Proposed GOA-FOPID.

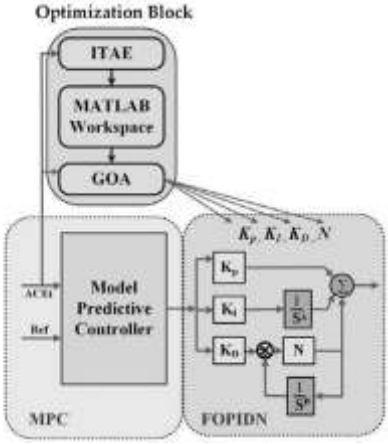

To address the LFC issue in dynamic load scenarios, the GOA-FOPID controller is suggested. By optimizing the suggested controller, GOA finds the optimal settings for the PI controller. An ideal signal is produced by cascading MPC and FOPID, which both have effective features on their own. The controller, filter, and model are the three main components of MPC. In the MPC scheme, control techniques are obtained by decreasing an objective function, and this is done by explicitly applying a prediction model of the system's response. The goal of optimization is to minimize the control effort within the defined restrictions and the discrepancy between the expected and reference responses. The MPC is shown to be just as effective as the optimum control. Computing efficiency, real-time applications, intrinsic delay correction, constraint handling, and future extension possibilities are its main strengths. Analyzing the system and predicting its real-time value is the primary goal of the MPC. In Figure 5, we can see the suggested controller architecture.

With PV system penetration in mind, the following state-space modeling is carried out for the power system model under study:

$$\frac{dx(t)}{dt} = Ax(t) + u(t) + B_l u_l(t),$$

$$y(t) = Cx(t).$$

From Equation above, $x(t)$ denotes the state vector, $u(t)$ the control vector, where the disturbance vector is represented by $u_l(t)$ and output system vector $y(t)$. System vectors are defined as:

$$x\ (t) = [\Delta P_1\ \Delta P_2\ \Delta P_{tie1}\ \Delta P_{tie2}\ \Delta F_1\ \Delta F_2\ \Delta P_{tie}$$

$$\Delta X_{g1} \Delta X_{g2}\ \Delta X_{t1}\ \Delta X_{t2}\ \Delta X_{r1}\ \Delta X_{r2}\ ]^T$$

$$u\ (t) = [\Delta P_{c1}\ \Delta P_{c2}]^T$$

$$u_f\ (t) = [\Delta P_{L1}\ \Delta P_{L2}]^T$$

$$y\ (t) = [\Delta ACE_1\ \Delta ACE_2]^T$$

$$A = \begin{bmatrix}
-a_1 & 0 & 0 & 0 & 0 & 0 & 0 & 0 & 0 & 0 & 0 & 0 & 0 \\
0 & -a_1 & 0 & 0 & 0 & 0 & 0 & 0 & 0 & 0 & 0 & 0 & 0 \\
(a_2 - a_1) & 0 & -a_1 & 0 & 0 & 0 & 0 & 0 & 0 & 0 & 0 & 0 & 0 \\
0 & (a_2 - a_1) & 0 & -a_1 & 0 & 0 & 0 & 0 & 0 & 0 & 0 & 0 & 0 \\
0 & 0 & 0 & 0 & -\frac{1}{M} & 0 & -\frac{D}{M} & 0 & 0 & 0 & 0 & \frac{D}{M} & 0 \\
0 & 0 & 0 & 0 & 0 & -\frac{1}{M} & \frac{D}{M} & 0 & 0 & 0 & 0 & 0 & \frac{D}{M} \\
0 & 0 & 0 & 0 & 2\Pi T_{12} & -2\Pi T_{12} & 0 & 0 & 0 & 0 & 0 & 0 & 0 \\
0 & 0 & 0 & 0 & -\frac{1}{RT_g} & 0 & 0 & -\frac{1}{T_g} & 0 & 0 & 0 & 0 & 0 \\
0 & 0 & 0 & 0 & 0 & -\frac{1}{RT_g} & 0 & 0 & -\frac{1}{T_g} & 0 & 0 & 0 & 0 \\
0 & 0 & 0 & 0 & -\frac{K_r T_r}{RT_g T_r} & 0 & 0 & -\frac{K_r T_r}{T_g T_r} & 0 & -\frac{1}{T_r} & 0 & 0 & 0 \\
0 & 0 & 0 & 0 & 0 & -\frac{K_r T_r}{RT_g T_r} & 0 & 0 & -\frac{K_r T_r}{T_g T_r} & 0 & \frac{1}{T_r} & 0 & 0 \\
0 & 0 & 0 & 0 & 0 & 0 & 0 & 0 & 0 & \frac{1}{T_t} & 0 & \frac{1}{T_t} & 0 \\
0 & 0 & 0 & 0 & 0 & 0 & 0 & 0 & 0 & 0 & \frac{1}{T_t} & 0 & \frac{1}{T_t}
\end{bmatrix}$$

$$\mathrm{B} = \begin{bmatrix}
K_1 & 0 \\
0 & K_1 \\
K_1 & 0 \\
0 & K_1 \\
0 & 0 \\
0 & 0 \\
0 & 0 \\
\frac{1}{T_g} & 0 \\
0 & \frac{1}{T_g} \\
\frac{K_r T_r}{T_g T_r} & 0 \\
0 & \frac{K_r T_r}{T_g T_r} \\
0 & 0 \\
0 & 0
\end{bmatrix} \quad B_f = \begin{bmatrix}
0 & 0 \\
0 & 0 \\
0 & 0 \\
0 & 0 \\
0 & 0 \\
0 & 0 \\
0 & 0 \\
\frac{-D}{M} & 0 \\
0 & \frac{-D}{M} \\
0 & 0 \\
0 & 0 \\
0 & 0 \\
0 & 0
\end{bmatrix}$$

$$C = \begin{bmatrix}
0 & 0 & 0 & 0 & 1 & B & 0 & 0 & 0 & 0 & 0 & 0 & 0 \\
0 & 0 & 0 & 0 & -1 & B & 0 & 0 & 0 & 0 & 0 & 0 & 0
\end{bmatrix}$$

After being translated into a discrete time space model, the equations provided above are expressed as

$$x\ (k+1) = A_d\ x\ (k) + B_d u\ (k) + B_{fd} u_f\ (k)$$

$$y\ (k) = Cx\ (k)$$

The above-mentioned change in equations may be expressed as

$$\Delta x\ (k+1) = A_d \Delta x\ (k) + B_d \Delta u\ (k) + B_{fd} \Delta u_f\ (k),$$

$$\Delta y\ (k) = C \Delta x\ (k).$$

The cost function that includes the MPC restriction is described for the LFC issue as

$$min_{\Delta u(k),\ldots,\Delta u(k+M-1)} \left\{ \sum_{j=0}^{m-1} \Delta u^T (k+j) R \Delta u (k+j) + \sum_{j=0}^{P-1} \Delta y^T (k+i) Q \Delta y (k+i) \right\}.$$

4. Results and Discussion

Table 1 compares the optimized controller parameters and performance indices for different control strategies applied to the two-area power system. The proposed GOA-FOPID controller exhibits improved tuning values of proportional, integral, derivative, and fractional orders in both areas when compared with FA-PI [48], FOPI-FOPIDN [49], ZOA-FOPID [50], and MOO-FOPID [51] approaches. The frequency deviation indices Δf_1 and Δf_2 are considerably lower with the proposed method, indicating superior disturbance rejection capability. Tie-line power deviation ΔP_{tie12} is also minimized, reflecting better coordination between the interconnected areas. The integral squared error value shows a substantial reduction to 13.916, confirming enhanced dynamic accuracy and faster damping characteristics. These results validate the effectiveness of GOA-FOPID in achieving reliable load frequency control performance.

Table 1: Controller Parameters and Performance Indices

Parameters	FA-PI [48]	FOPI-FOPIDN [49]	ZOA-FOPID [50]	MOO-FOPID [51]	Proposed GOA-FOPID
Area-1	K_p = 1.294 K_i = 0.0227	K_p = 1.4610 K_i = 0.3162 K_d = 0.7831	K_p = 0.8093 K_i = 0.7987	K_p = 1.0616 K_i = 0.8275 K_d = 0.3040 N = 129.676	K_p = 1.3232 K_i = 0.3878 K_d = 0.7291 λ = 0.1467 μ = 0.1617 N = 141.65
Area-2	K_p = 1.429 K_i = 0.0579	K_p = 1.4127 K_i = 0.1762 K_d = 0.2033	K_p = 0.7972 K_i = 0.7855	K_p = 1.5410 K_i = 0.8763 K_d = 0.2194 N = 134.12	K_p = 1.3855 K_i = 0.3490 K_d = 0.2752 λ = 0.3040 μ = 0.1665 N = 139.25
Δf_1	22.60	5.438	4.40	2.138	1.362
ΔP_{tie12}	23.65	5.562	4.64	2.54	1.954
Δf_2	21.21	5.291	4.38	2.501	1.91
ISE $\times 10^{-3}$	120.171	81.068	43.111	36.659	13.916

Figure 6(a) illustrates the frequency deviation response Δf_1 of area one under scenario one for different controllers. The proposed GOA-FOPID controller achieves faster damping of oscillations and reaches steady state in shorter time compared with FOPI-FOPIDN, ZOA-FOPID, and MOO-FOPID methods. The peak undershoot and overshoot values are significantly reduced, indicating better stability of the system. The response curve of GOA-FOPID remains close to zero after a brief transient period, demonstrating superior disturbance rejection capability in area one.

Figure 6: Responses for Scenario 1 (a) Δf_1, (b) ΔP_{tie12}, (c) Δf_2.

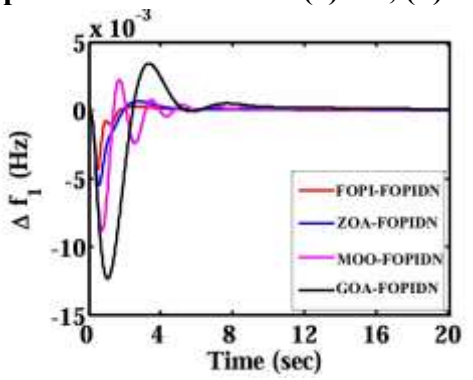

(a)

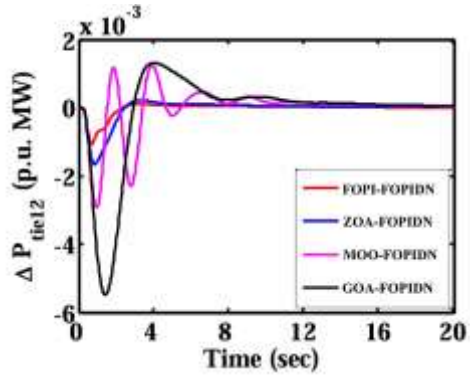

(b)

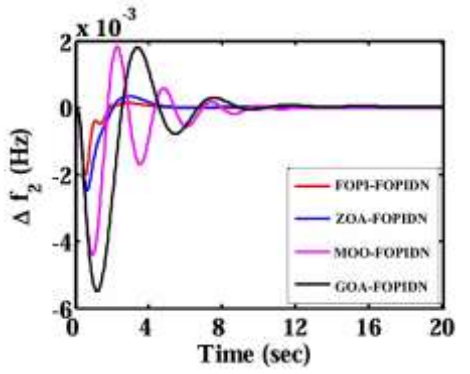

(c)

Figure 6(b) presents the tie-line power deviation ΔP_{tie12} between the two interconnected areas. The GOA-FOPID controller provides quicker restoration of tie-line power with minimal oscillatory behaviour. Competing controllers exhibit larger deviations and longer settling durations. The proposed approach limits the magnitude of initial power fluctuation and ensures smooth power exchange between areas. The reduced amplitude of oscillations confirms enhanced coordination and effective control action

achieved through fractional order optimization. Figure 6(c) shows the frequency deviation Δf_2 of area two for scenario one. The GOA-FOPID controlled response demonstrates rapid convergence to nominal frequency with very small steady state error. Other techniques display higher oscillations and delayed stabilization. The proposed controller effectively suppresses the impact of load perturbation on area two and maintains frequency within acceptable limits. The smoother response curve reflects improved robustness and dynamic performance of the fractional order controller in the interconnected system.

Figure 7: Responses for Scenario 2 (a) Δf_1, (b) ΔP_{tie12}, (c) Δf_2.

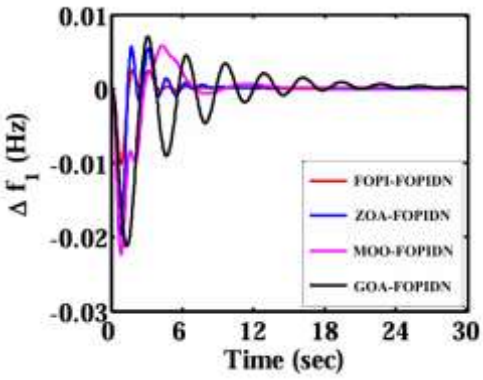

(a)

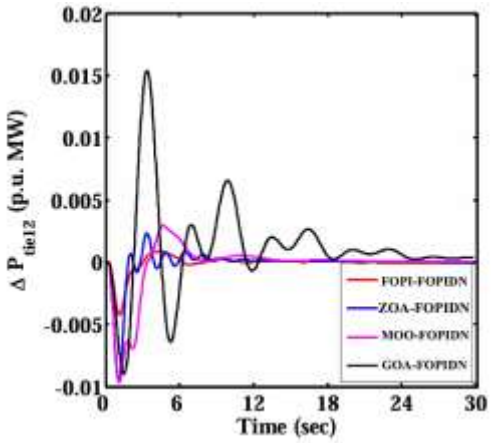

(b)

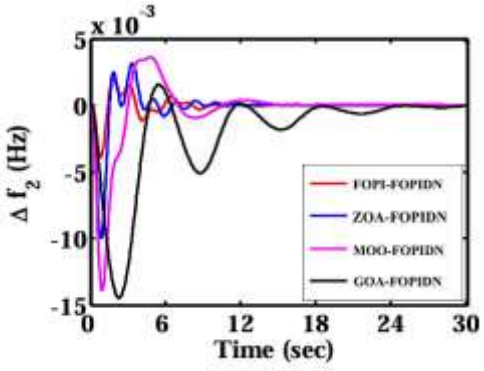

(c)

Figure 7(a) represents the frequency deviation Δf_1 of area one under scenario two for different control strategies. The GOA-FOPID controller demonstrates quicker suppression of oscillations and attains steady state earlier than FOPI-FOPIDN, ZOA-FOPID, and MOO-FOPID controllers. The magnitude of

initial undershoot is comparatively lower with the proposed method, indicating better stability margin. The response curve remains close to nominal frequency after a short transient duration, confirming the effectiveness of fractional order tuning in maintaining frequency regulation.

Figure 7(b) illustrates the tie-line power deviation ΔP_{tie12} between the two areas for scenario two. The GOA-FOPID controller limits the amplitude of power oscillations and restores tie-line power more rapidly than the other controllers. The competing methods show prolonged fluctuations and higher peak deviations. The proposed technique ensures smoother power exchange and enhanced coordination between the interconnected regions. The improved damping characteristic reflects the capability of the optimized fractional controller in handling load disturbances. Figure 7(c) shows the frequency deviation Δf_2 of area two for scenario two. The GOA-FOPID response converges to zero faster and exhibits reduced oscillatory behaviour compared with FOPI-FOPIDN, ZOA-FOPID, and MOO-FOPID approaches. The peak deviation is minimized, demonstrating strong disturbance rejection in area two. The smooth trajectory of the proposed controller indicates superior dynamic stability and robustness under renewable integrated conditions. The results validate the suitability of GOA-FOPID for effective load frequency control.

Table 2 presents the settling time and error performance of different controllers for scenario one and scenario two. The proposed GOA-FOPID controller achieves the shortest settling times for frequency deviations Δf_1 and Δf_2 as well as for tie-line power deviation ΔP_{tie12} in both scenarios. In scenario one, the GOA-FOPID reduces settling time to 6.132 s for Δf_1 and 5.534 s for Δf_2, which is considerably lower than the other methods. Similar improvement is observed in scenario two where the proposed controller maintains faster stabilization under larger disturbances. The integral squared error values are also minimum with GOA-FOPID, confirming superior dynamic accuracy and effective damping capability.

Table 2: Settling time of the system responses for scenario 1 and 2.

Settling Time (Sec)		FOPI-FOPIDN [49]	ZOA-FOPID [50]	MOO-FOPID [51]	Proposed GOA-FOPID
Scenario 1	Δf_1	17.57	14.95	9.772	6.132
	ΔP_{tie12}	18.45	15.17	9.88	6.75
	Δf_2	16.14	13.29	9.78	5.534
	ISE $\times 10^{-3}$	21.665	18.202	15.653	11.926
Scenario 2	Δf_1	32.13	17.39	14.14	9.786
	ΔP_{tie12}	31.99	17.32	14.73	10.28
	Δf_2	31.34	20.19	14.94	9.95
	ISE $\times 10^{-3}$	47.866	41.336	36.405	26.752

5. Conclusion and Future scope

The research investigated load frequency control of a renewable integrated two-area power system using a GOA optimized fractional order PID controller. The developed model considered photovoltaic generation in area one and wind generation in area two along with virtual inertia support to emulate conventional generator behaviour. Comparative analysis with existing controllers confirmed that the

proposed technique provides faster damping of frequency and tie-line power oscillations under different disturbance conditions. The settling time and integral squared error were considerably reduced, indicating improved dynamic accuracy and robustness. The fractional order structure offered additional tuning flexibility, enabling better adaptation to low inertia characteristics of renewable sources. The results established that the GOA-FOPID controller maintains system frequency closer to nominal value and ensures effective coordination between interconnected areas. The proposed approach can be extended to multi-area smart grids and real-time hardware implementation for practical deployment. Perhaps in the future, when designing LFC schemes for more complicated, contemporary, linked power systems, this research will take system latency into account and use updated optimization approaches.

6. References

1. Khodabakhshian, A., &Hooshmand, R. (2009). A new PID controller design for automatic generation control of hydro power systems. *International Journal of Electrical Power & Energy Systems*, *32*(5), 375–382. https://doi.org/10.1016/j.ijepes.2009.11.006
2. Hsu, Y., & Chan, W. (1984). Optimal variable structure controller for the load-frequency control of interconnected hydrothermal power systems. *International Journal of Electrical Power & Energy Systems*, *6*(4), 221–229. https://doi.org/10.1016/0142-0615(84)90004-8
3. Ikhe, A., &Kulkarni, A. (2013). Load frequency control for two area power system using different controllers. *International Journal of Advances in Engineering & Technology*, *6*(4), 1796-1802.
4. Rajamand, S. (2021). Load frequency control and dynamic response improvement using energy storage and modeling of uncertainty in renewable distributed generators. *Journal of Energy Storage*, *37*, 102467. https://doi.org/10.1016/j.est.2021.102467
5. Tan, K. M., Babu, T. S., Ramachandaramurthy, V. K., Kasinathan, P., Solanki, S. G., &Raveendran, S. K. (2021). Empowering smart grid: A comprehensive review of energy storage technology and application with renewable energy integration. *Journal of Energy Storage*, *39*, 102591. https://doi.org/10.1016/j.est.2021.102591
6. Peddakapu, K., Mohamed, Sulaiman, M., Srinivasarao, P., Veerendra, A., & Leung, P. (2020). Performance analysis of distributed power flow controller with ultra-capacitor for regulating the frequency deviations in restructured power system. *Journal of Energy Storage*, *31*, 101676. https://doi.org/10.1016/j.est.2020.101676
7. Bevrani, H., Ghosh, A., &Ledwich, G. (2010). Renewable energy sources and frequency regulation: survey and new perspectives. *IET Renewable Power Generation*, *4*(5), 438–457. https://doi.org/10.1049/iet-rpg.2009.0049
8. Ibraheem Kumar P, Kothari DP (2005) Recent philosophies of automatic generation control strategies in power systems. *IEEE* Trans Power Syst 20(1):346–357
9. Cohn N (1967) Considerations in the regulation of interconnected areas. IEEE Trans Power ApparSyst PAS-86(12):1527–1538
10. Quazza, G. (1966). *Noninteracting controls of interconnected electric power systems*. https://www.semanticscholar.org/paper/Noninteracting-Controls-of-Interconnected-Electric-Quazza/7578617f7ddbdaa742046d6764b812592348b679
11. Kwatny, H., Kalnitsky, K., & Bhatt, A. (1975). An optimal tracking approach to load-frequency control. *IEEE Transactions on Power Apparatus and Systems*, *94*(5), 1635–1643. https://doi.org/10.1109/t-pas.1975.32006

12. Saha D, Saikia LC (2017) Performance of FACTS and energy storage devices in a multi area wind–hydro–thermal system employed with SFS optimized I-PDF controller. J Renew Sustain Energy 9:024103. https://doi.org/10.1063/1.4980160
13. Babu, N. R., Bhagat, S. K., Saikia, L. C., Chiranjeevi, T., Devarapalli, R., &Márquez, F. P. G. (2022). A comprehensive review of recent strategies on Automatic Generation Control/Load Frequency Control in Power Systems. *Archives of Computational Methods in Engineering*, *30*(1), 543–572. https://doi.org/10.1007/s11831-022-09810-y
14. Arulkumar K, Vijayakumar D, &Palanisamy K. (2016). Recent advances and control techniques in grid connected PV system â€“ A review. *International Journal of Renewable Energy Research (IJRER)*, *6*(3), 1037–1049. https://www.ijrer.com/index.php/ijrer/article/view/4075
15. Arulkumar, K., Vijayakumar, D., & Palanisamy, K. (2014). Efficient control design for single phase grid tie inverter of PV system. *2014 International Conference on Advances in Electronics Computers and Communications*, 1–6. https://doi.org/10.1109/icaecc.2014.7002461
16. Wooding B., Lavaei A., Soudjani S. Formal control of new England 39-bus test system: an assume-guarantee approach. *arXivpreprint* arXiv:2307.03467 2023.
17. B. Alghamdi, C.A. Canizares, ˜ Frequency regulation in isolated microgrids through optimal droop gain and voltage control, *IEEE Trans*. Smart Grid 12 (2) (2020) 988–998
18. Masikana, S., Sharma, G., & Sharma, S. (2024). Renewable energy sources integrated load frequency control of power system: A review. *e-Prime - Advances in Electrical Engineering Electronics and Energy*, *8*, 100605. https://doi.org/10.1016/j.prime.2024.100605
19. Monje, C. A., Vinagre, B. M., Feliu, V., & Chen, Y. (2008). Tuning and auto-tuning of fractional order controllers for industry applications. *Control Engineering Practice*, *16*(7), 798–812. https://doi.org/10.1016/j.conengprac.2007.08.006
20. Y. Chen, I. Petras, and D. Xue, ‘‘Fractional order control—A tutorial,’’ in Proc. Amer. Control Conf., Jun. 2009, pp. 1397–1411.
21. C. Monje, Y. Chen, B. Vinagre, D. Xue, and V. Feliu, Fractional Order Systems and Control—Fundamentals and Applications (Advances in Industrial Control). London, U.K.: Springer-Verlag, 2010, doi: 10.1007/978-1-84996-335-0.
22. Pullaguram, D., Mukherjee, M., Mishra, S., & Senroy, N. (2016). *Non-linear fractional order controllers for autonomous microgrid system*. https://www.semanticscholar.org/paper/Non-linear-fractional-order-controllers-for-system-Pullaguram-Mukherjee/c2343e95e08379717a192aab6d986c15ca1cf16c
23. Balaska, H., Ladaci, S., Schulte, H., & Djouambi, A. (2019). Adaptive cruise control system for an electric vehicle using a fractional order model Reference Adaptive Strategy. *IFAC-PapersOnLine*, *52*(13), 194–199. https://doi.org/10.1016/j.ifacol.2019.11.096
24. Zhu, D., Liu, L., & Liu, C. (2014). Optimal fractional-order PID control of chaos in the fractional-order BUCK converter. *2014 9th IEEE Conference on Industrial Electronics and Applications*, 787–791. https://doi.org/10.1109/iciea.2014.6931269
25. Caponetto, R., Dongola, G., Fortuna, L., & Petráš, I. (2010). Fractional Order Systems. *World Scientific Series on Nonlinear Science Series A*. https://doi.org/10.1142/7709
26. Miller, K., & Ross, B. (1993). *An introduction to the fractional calculus and fractional differential equations*. https://www.semanticscholar.org/paper/An-Introduction-to-the-Fractional-Calculus-and-Miller-Ross/d1ada669360efa7be4cbba3c50f414bcf864d6f3

27. Y. Chen, I. Petras, and D. Xue, ‘‘Fractional order control—A tutorial,’’ in Proc. Amer. Control Conf., Jun. 2009, pp. 1397–1411.
28. Warrier, P., & Shah, P. (2021). Fractional order control of power electronic converters in industrial drives and renewable energy systems: a review. *IEEE Access*, *9*, 58982-59009.
29. A. Loverro, ‘‘Fractional calculus: History, definitions and applications for the engineer,’’ Univ. Notre Dame, Notre Dame, IN, USA, Tech. Rep., 2004.
30. B. Vinagre, I. Podlubny, A. Hernández, and V. Feliu, ‘‘Some approximations of fractional order operators used in control theory and applications,’’ Fractional Calculus Appl. Anal., vol. 3, no. 3, pp. 231–248, Jan. 2000.